

Lawrence Berkeley National Laboratory

Recent Work

Title

PRODUCTION OF STRANGE PARTICLES IN HADRONIZATION PROCESSES

Permalink

<https://escholarship.org/uc/item/4z82h43k>

Author

Hofmann, W.

Publication Date

1987-08-01

c.2



Lawrence Berkeley Laboratory

UNIVERSITY OF CALIFORNIA

Physics Division

Presented at the International Symposium on
Strangeness in Hadronic Matter,
Bad Honnef, West Germany, June 1-5, 1987

Production of Strange Particles in Hadronization Processes

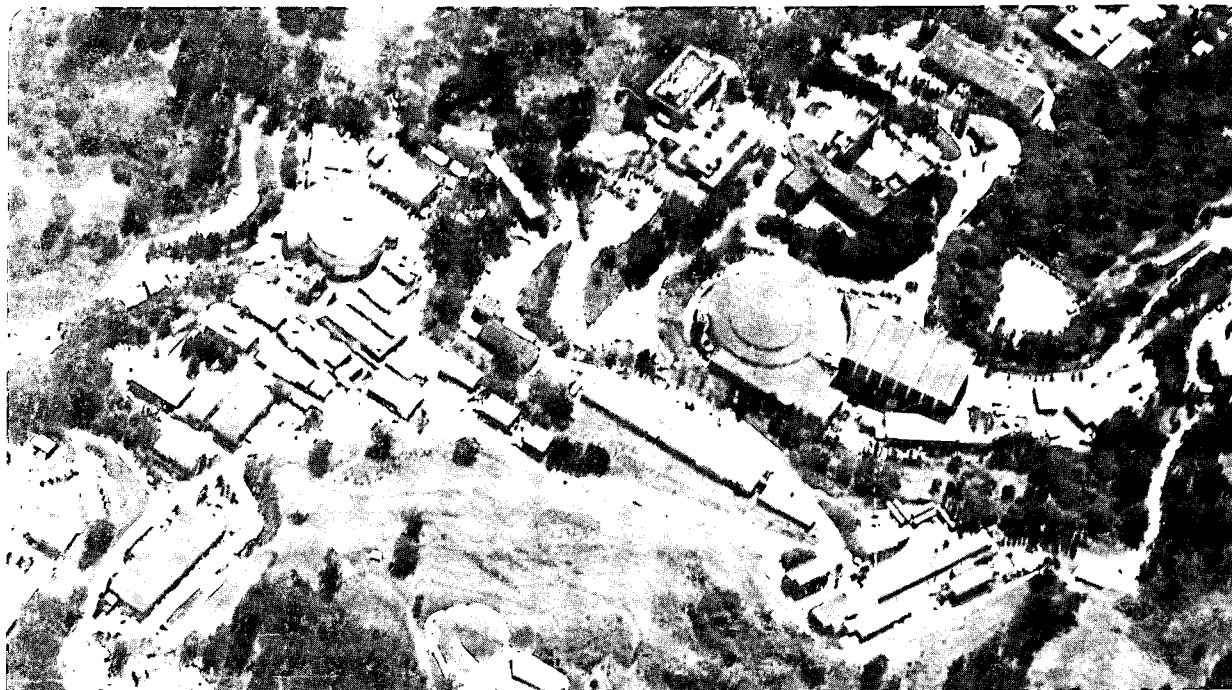
W. Hofmann

August 1987

RECEIVED
LAWRENCE
BERKELEY LABORATORY

OCT 29 1987

LIBRARY AND
DOCUMENTS SECTION



LBL-23921

c.2

DISCLAIMER

This document was prepared as an account of work sponsored by the United States Government. While this document is believed to contain correct information, neither the United States Government nor any agency thereof, nor the Regents of the University of California, nor any of their employees, makes any warranty, express or implied, or assumes any legal responsibility for the accuracy, completeness, or usefulness of any information, apparatus, product, or process disclosed, or represents that its use would not infringe privately owned rights. Reference herein to any specific commercial product, process, or service by its trade name, trademark, manufacturer, or otherwise, does not necessarily constitute or imply its endorsement, recommendation, or favoring by the United States Government or any agency thereof, or the Regents of the University of California. The views and opinions of authors expressed herein do not necessarily state or reflect those of the United States Government or any agency thereof or the Regents of the University of California.

Production of Strange Particles in Hadronization Processes

W. Hofmann

Lawrence Berkeley Laboratory
University of California
Berkeley, CA 94720

August 1987

Invited Talk at the
International Symposium on Strangeness in Hadronic Matter
1-5 June 1987, Bad Honnef, FRG

Strange particles provide an important tool for the study of the color confinement mechanisms involved in hadronization processes. We review data on inclusive strange-particle production and on correlations between strange particles in high-energy reactions, and discuss phenomenological models for parton fragmentation.

1. INTRODUCTION.

Purpose of this paper is to review data and models on the production of strange particles in high-energy reactions such as hadron-hadron collisions, deep-inelastic lepton-hadron scattering and electron-positron annihilation. For the cases discussed in the following, the center-of-mass energy of the reaction is typically much larger than strange-hadron masses, and the production rates of strange particles should reflect the dynamics of the strong interaction rather than phase space constraints.

Since so far most talks at this conference have dealt with strangeness in nuclear physics, I would like to review briefly the phenomenology of high-energy reactions and point out some of the reasons why production rates and production characteristics of strange particles are of considerable interest. Probably the most typical feature of high-energy reactions is the formation of jets, i.e. the emission of particles in well-collimated bundles. In electron-positron annihilation into hadrons in the PEP/PETRA energy range, for example, one typically finds two jets recoiling against each other, as exemplified by the "typical" event shown in Fig. 1. Of course, the two jets reflect the production of a primary quark-antiquark pair by a virtual photon; as the two quarks recede from each other, a confining color force field coupled to their SU(3) color charges prevents them from escaping as asymptotic particles and instead results in the production of jets of hadrons collimated around the parton directions.

The mechanism of color confinement is one of the big open questions in particle physics and has attracted considerable attention, so far without complete success. The study of hadronization processes in general, and of strange-particle production in particular

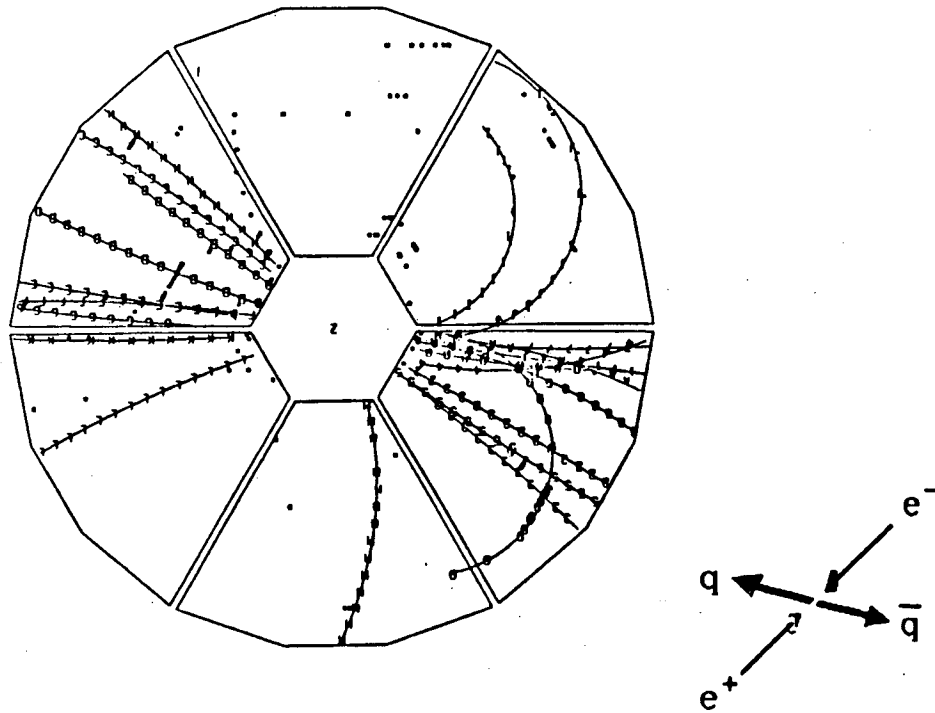


FIGURE 1
 A typical 2-jet event in e^+e^- annihilation at $\sqrt{s} = 29$ GeV, viewed along the e^+e^- collision axis.

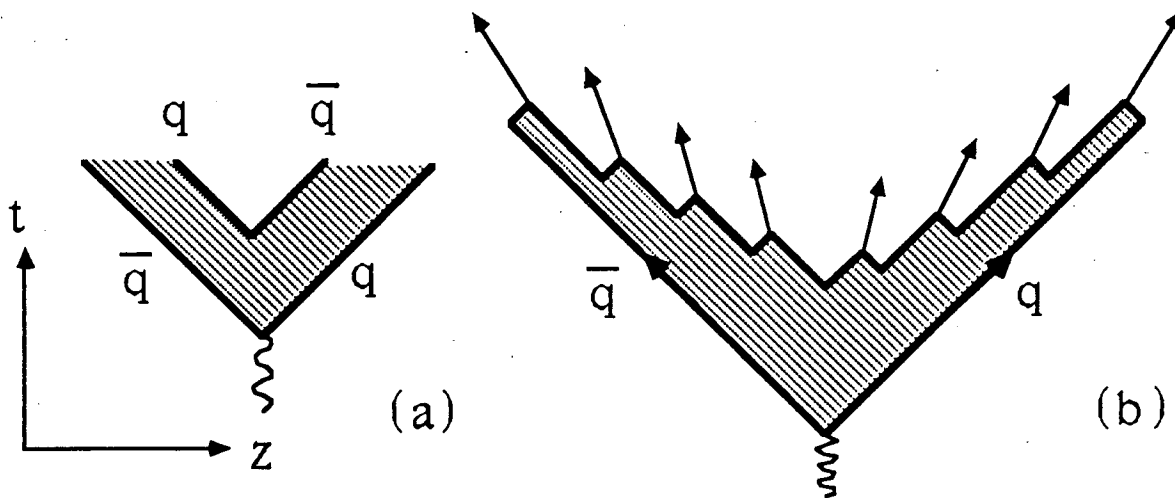


FIGURE 2
 Particle production in the constant color force field between quark and antiquark: (a) production of a new quark-antiquark pair; (b) a complete annihilation event. Since the creation of a new quark pair will on average occur after a constant proper time, particle production points are scattered about a space-time hyperbola.

provides one of the handles towards a deeper understanding of the strong forces responsible for confinement:

- It is presently believed that the confining potential between a quark and an antiquark rises linearly with distance, i.e. the force field can be pictured as a basically one-dimensional field, a "color flux tube" or "string", often compared to vortex lines in a superconductor. In such a model¹⁻⁵, confinement arises since once the primary quarks are separated by a certain distance (of the order of one fermi), it is energetically favorable to form a new quark-antiquark pair which screens the color field (Fig. 2(a)). At high energies, the process is repeated several times until the mass of each quark-antiquark system joined by a string piece is consistent with typical meson masses (Fig. 2(b)). In such a process, the rate of strange quark production as compared to production rates for light up or down quarks depends on the energy density in the color field^{2,4-7}. The ratio of strange to up or down quark rates provides therefore a measurement of this energy density, the "string constant", or in other words of the typical scales of space, time and momentum transfer involved in confinement processes.
- The strangeness quantum number can also be used as a tracer to explore reaction dynamics. In a typical high-energy reaction, 10 or more pions are produced in the confinement process, but typically only one or two pairs of strange particles. The position in phase-space of a strange hadron with respect to its associated anti-strange partner provides clues to the momentum transfers in the confinement process (Fig. 3). In this context, it is also helpful that there are few resonances decaying into pairs of strange particles, whereas the observed correlations between pions are largely caused by resonance decays.
- In general strange particles, because of their larger masses, make a more reliable probe of the fragmentation process. Most pions stem from resonance decays. Since in a typical pion producing decay such as $\rho \rightarrow \pi\pi$ the Q-value of the decay is larger than the pion mass, the momentum of the final-state pion is a very poor

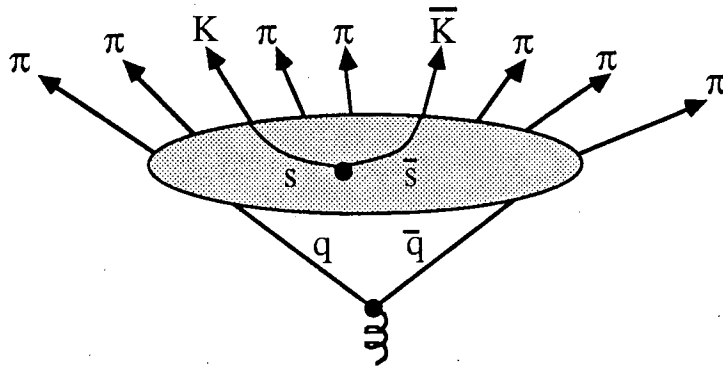


FIGURE 3

The strangeness quantum number can be used to label pairs of hadrons containing pair-produced quarks. The four-momentum difference of those hadrons measures the typical scale of momentum transfer in the confinement process.

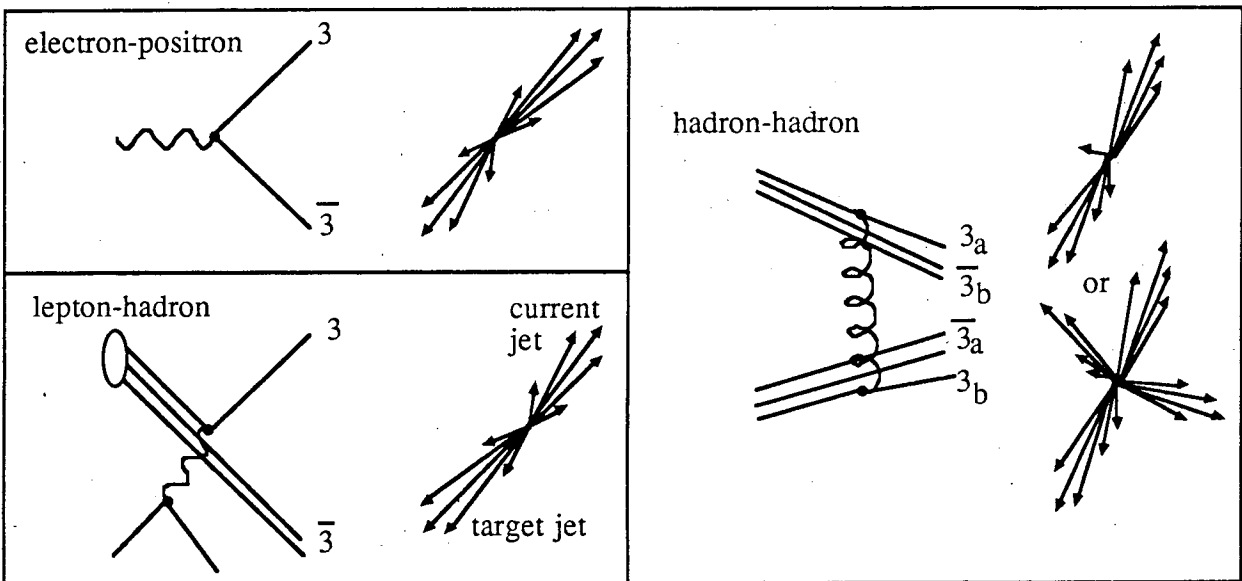


FIGURE 4

Underlying partonic processes in high energy reactions and the resulting jet structures of the events: (a) e^+e^- annihilation into two jets; (b) lepton-nucleon scattering with current jet and target jet; (c) hadron-hadron collisions. For large momenta of the exchanged gluon, a four-jet structure is visible, corresponding to the four color triplets created in the process. For small momenta, pairs of jets coalesce. (Another possible process is of course the scattering off gluons.)

estimator of its parent's momentum. This situation improves as we go to strange mesons. (E.g. consider $K^* \rightarrow K\pi$.)

- Whereas meson production appears very natural in most models of the confinement mechanism, the mechanisms responsible for baryon production are by no means obvious^{8,9}. Baryon production rates, with the number of strange quarks in the baryon between 0 and 3, provide an excellent testing ground for models and allow systematic studies.
- Finally, strange baryons enable us to study polarization effects in the hadronization process. In particular, the Λ baryon polarization is easy to measure and provides a direct measurement of the polarization of the s-quark. String models, for example, do predict a significant polarization of secondary quarks produced in the color field¹⁰.

It is believed that the separation of color charges, followed by a confinement process resulting in a two- or multijet structure is one of the fundamental mechanisms of particle production in high-energy reactions¹¹. Fig. 4 indicates the underlying processes in various reactions: e^+e^- annihilation into quark and antiquark, resulting usually in a two-jet event; deep-inelastic lepton nucleon scattering where a quark is scattered out of a nucleon and where the remaining diquark acts as a color-antitriplet, resulting in a current jet and a target jet; finally hadron-hadron collisions, where the underlying mechanism is not really known, but a reasonable (somewhat simplified) guess is that a gluon is exchanged, giving rise to two triplet-antitriplet systems and hence four jets. For low momentum transfers, pairs of jet overlap and we are left with a beam and a target jet. For high momenta of the exchanged gluon, a four jet structure is predicted and indeed observed.

The kinematics of particles within jets are typically described using a transverse variable, such as the transverse momentum with respect to the jet axis, and a longitudinal variable such as the rapidity y :

$$y = \frac{1}{2} \log \left(\frac{E+p_{\parallel}}{E-p_{\parallel}} \right).$$

Rapidity is basically the relativistic equivalent of the velocity β in non-relativistic systems: rapidity differences are invariant under longitudinal boosts, and particles from the decay of a common parent have the same average rapidity and typically a small rapidity difference of $O(1)$. Furthermore, a small rapidity range dy corresponds to the volume element dp/E of Lorentz invariant longitudinal phase space. It is therefore not surprising that particles in jets exhibit a basically flat distribution in rapidity, falling off near the kinematic limits. For example, in e^+e^- annihilation at PEP or PETRA energies, the kinematically allowed range for pions is ± 5 units in rapidity; one finds¹² a central plateau of ± 2 units, followed by "fragmentation regions" at both ends (Fig. 5). The fragmentation regions are populated mainly by particles containing the initial parton(s), i.e. either the primary quark or the anti-quark in the case of e^+e^- annihilation. The central region contains mainly particles made of newly formed quarks. A very clear example for the distinction between central region and fragmentation region is given by pp interactions¹³ (Fig. 6): in the central region of about ± 2 units in rapidity, the average charge of hadrons is close to zero, indicating that they do not contain valence quarks of the incoming protons. At higher rapidity, we find the remnants of the beam protons, resulting in a positive average charge of the produced particles. Here, we will concentrate on the central region. With the exception of lepton-nucleon scattering, the fragmentation regions are of limited use for the study of strangeness production: in e^+e^- annihilation, strange particle production in these regions is dominated by decay products of charmed and bottom hadrons, and in hadronic reactions the fragmentation regions usually contain complicated multi-parton systems.

In the main body of this paper, I will address the following topics:

- Strangeness suppression in hadronization processes and its phenomenological interpretation
- Correlations between strange particles and study of particle production mechanisms
- Production of strange baryons.

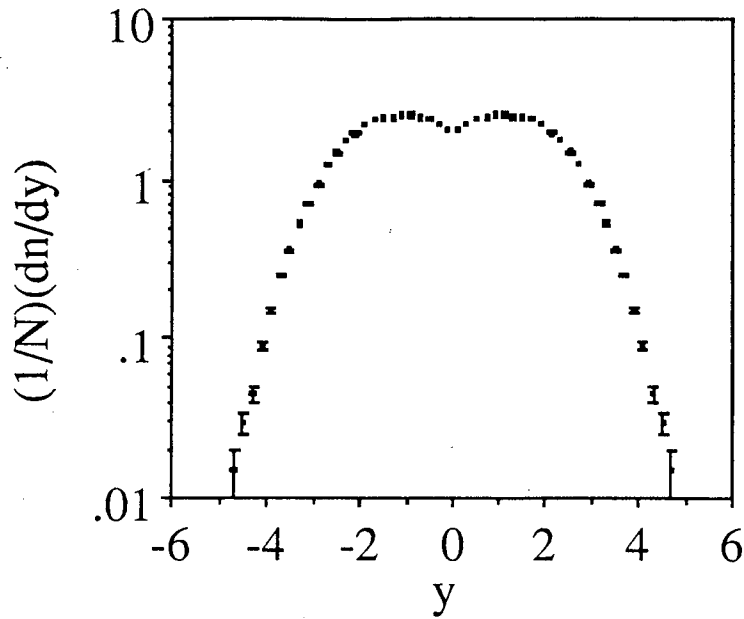
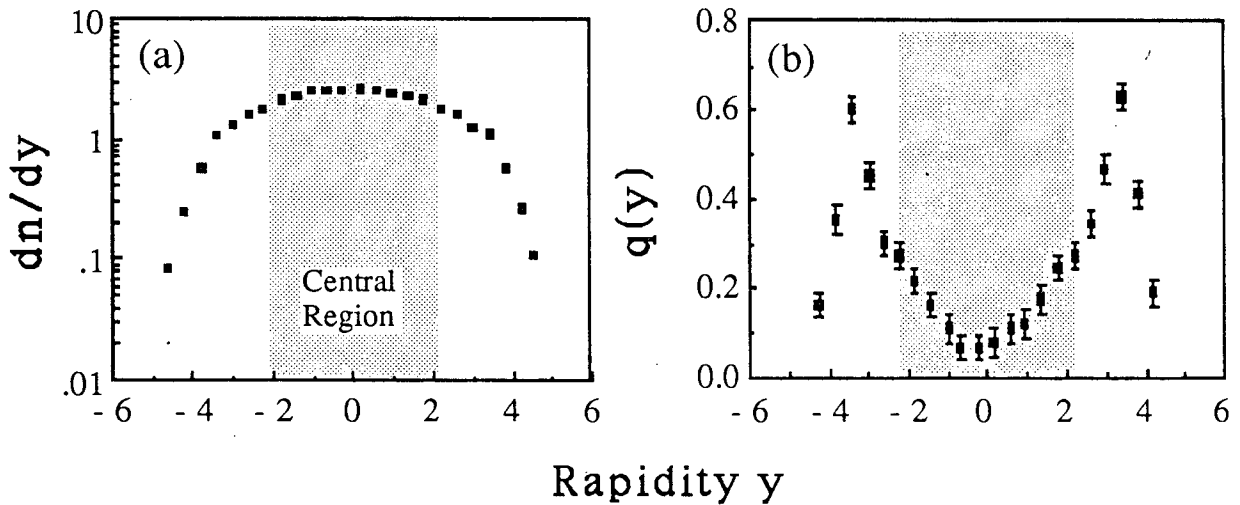


FIGURE 5

Rapidity distribution of charged hadrons in e^+e^- annihilation at $\sqrt{s} = 34 \text{ GeV}^{12}$. The dip at $y \approx 0$ is largely due to a bias introduced by the algorithm used to define the jet axis (thrust axis).



FFIGURE 6

(a) Rapidity distribution of charged hadrons in proton-proton collisions at $\sqrt{s} = 52 \text{ GeV}^{13}$. (b) Net charge density, i.e. number of positive hadrons minus number of negative hadrons per unit of rapidity.

2. STRANGENESS SUPPRESSION

One of the first observations concerning the production of strange particles in hadronization processes was a breaking of SU(3) symmetry, as indicated by a reduction in the yields of strange hadrons as compared to non-strange particles. Figs. 7 (a) and (b) show the inclusive production cross sections for pions and for charged and neutral kaons (a) and for pions, protons, lambdas and xi's (b), for e^+e^- annihilation at 34 GeV center-of-mass energy as a function of $x = 2E_{\text{hadron}}/\sqrt{s}$ ¹⁴. Both for mesons and baryons it is obvious that production cross sections decrease with increasing number of strange quarks in a hadron. Phenomenologically, this behavior can be accounted for by introduction of a suppression factor λ for the production probability $P(s\bar{s})$ of strange quark-antiquark pairs in the color field, as compared to light (up or down) pairs:

$$\lambda = \frac{P(s\bar{s})}{P(u\bar{u})} = \frac{P(s\bar{s})}{P(d\bar{d})} \quad (1)$$

(As we shall see later, the energy density in the color field is too small to produce $c\bar{c}$ or $b\bar{b}$ pairs at any appreciable rate.) Assuming that meson production can indeed be described as a two-step process - quark-antiquark pair production followed by a flavor-independent recombination into mesons - and neglecting leading-particle effects, we can express the rate of primary mesons with open strangeness in terms of λ :

$$\frac{P(\text{strange meson})}{P(\text{non-strange meson})} = \frac{4\lambda}{4+\lambda^2} \quad (2).$$

Note, however, that Eqn. (2) holds only for primary particles; the stable hadrons observed in the detector result largely from resonance decays which produce many new pions, but usually don't change the number of strange hadrons. Correspondingly, the ratio of final kaons to pions differs significantly from the prediction of Eqn. (2), and depends on assumptions concerning the primary hadrons, such as the ratio of vector mesons to pseudoscalar mesons. This fact complicates the experimental determination of λ tremendously. One now has to solve the matrix equation

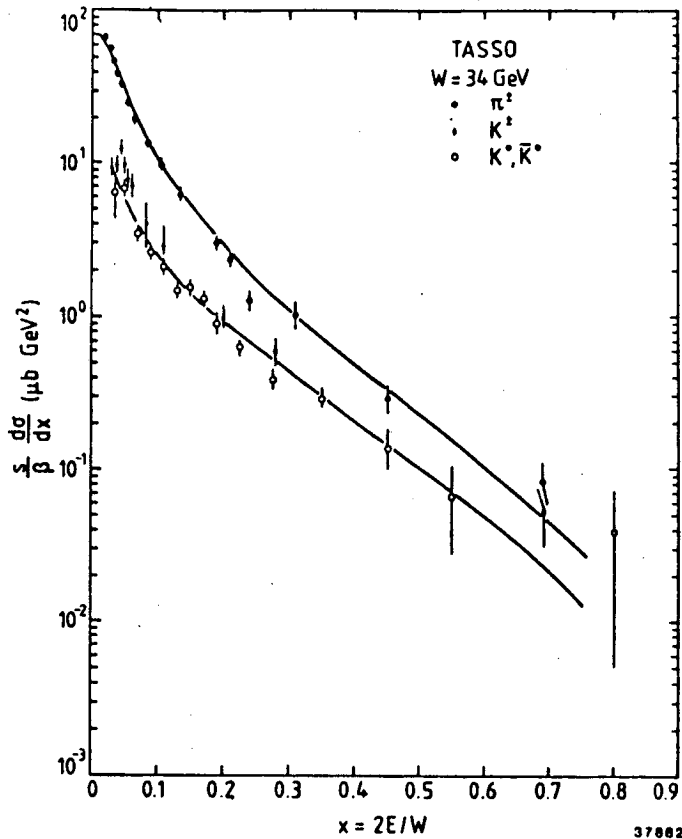
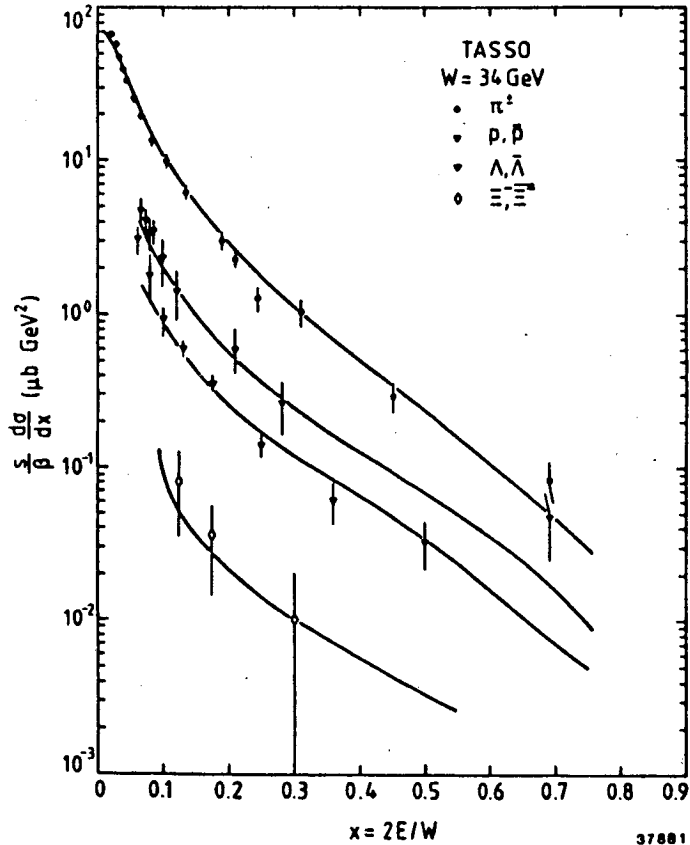


FIGURE 7
 (a) Scaled cross section $(s/\beta)(d\sigma/dx)$ for production of charged pions and kaons and of neutral kaons in e^+e^- annihilation at $\sqrt{s} = 34 \text{ GeV}$, as a function of $x = 2E/\sqrt{s}$. (b) Scaled cross section for production of pions, protons, lambdas and cascade particles. The curves show predictions of the Lund fragmentation model, with parameters optimized for best fit to the data.



$$\begin{pmatrix} \text{observed strange rate} \\ \text{observed non-str. rate} \end{pmatrix} = \begin{pmatrix} \approx 1 & \approx 0 \\ \alpha & \beta \end{pmatrix} \begin{pmatrix} \text{prim. strange rate} \\ \text{prim. non-str. rate} \end{pmatrix} \quad (3);$$

the matrix element α gives the average number of stable non-strange hadrons generated in the decay chain of a strange primary hadron, and β gives the number from non-strange primary hadrons. Unfortunately, the nature and composition of the primary hadrons are generally not well known, and one has to rely on assumptions. Often, the quark-model meson and baryon ground states are used to represent primary particles, i.e. pseudoscalar and vector mesons and octet and decuplet baryons are included. For the production rates SU(6) symmetry is assumed, broken by the additional strangeness suppression λ (and sometimes by additional spin- and flavor-dependent factors), and usually supplemented by a model for baryon production. The range of models is enormous - at one end the simple one-parameter (λ) statistical model¹⁵ (which tends to overestimate vector meson rates, indicating the need for a spin-dependent SU(6) breaking); at the other end the Lund Monte Carlo model⁵ with its about a dozen parameters related to the composition of primaries. Some authors include tensor mesons among primaries; nobody so far has consistently included $J^{PC} = 0^{++}, 1^{++}$ and 1^{+-} mesons, given that those multiplets are not even unambiguously established. Some recent models¹⁶⁻¹⁹ of parton fragmentation postulate "clusters" (i.e. highly excited meson states in the 1-3 GeV mass region, somewhat along the lines of Hagedorn's statistical bootstrap²⁰) as the primary objects produced in the process of color confinement and yield quite different values of λ .

Even once the definition of a primary particle is settled, there are still many choices. One can e.g. determine λ by twiddling the corresponding parameter(s) in a Monte Carlo event generator or an analytical model, until agreement with the data is reached, or one can use the model to isolate channels or kinematic regions where the relation between measured rates and λ is very direct and where corrections are believed to be small. For example, one should not have to worry about resonance decay products near the phase space limit $E_{\text{hadron}} \rightarrow \sqrt{s}/2$. In the analysis of data at lower cms ener-

gies, one has to decide whether the reduced phase space for strange particles should be included in the definition of λ or not. Other uncertainties concern the data used - one can use production cross sections in the central region, inclusive cross sections as a function of momentum, or just total multiplicities, and one can rely on some selected particle ratios (e.g. K/π) or instead aim for a global description of all observed cross sections.

Ideally, of course, all methods should yield the same λ ; in reality, however, no model describes the data perfectly, and the answers do vary by ± 20 to $\pm 30\%$, depending on the analysis technique. Let me substantiate this statement with a few examples: Fig. 8 shows the predicted K^\pm/π^\pm ratio as a function of λ , for models based on SU(6) symmetry with an additional vector meson suppression factor. Baryon production follows the Lund scheme⁵ and contains additional parameters. Curves shown are for vector/pseudoscalar = 0, 1:1, 3:1 and 1. The 3:1 case is essentially equivalent to the one-parameter additive quark model¹⁵; 1:1 is favored by data on ρ and K^* cross sections. We see that the ratio $(d\sigma/dy)_{K^\pm}/(d\sigma/dy)_{\pi^\pm} \approx (9.9 \pm 1.0)\%$ ³⁴ observed in the central rapidity region of high-energy e^+e^- annihilation corresponds to $\lambda \approx 0.2-0.3$, depending on the assumption concerning the vector/scalar ratio.

Moreover, analytical calculations of particle rates often differ significantly from the results obtained by a full Monte-Carlo implementation. Most fragmentation models predict that in the fragmentation region of a d quark (e.g. from νp scattering) $K^0/\pi^- = \lambda$ for large $x = 2E/\sqrt{s}$. A Monte Carlo simulation however demonstrates that corrections are non-negligible, in particular at the low \sqrt{s} values typical for neutrino experiments (Fig. 9 (a)).

An apparently less model-dependent technique was used in a summary by Wroblewski²¹: he simply counts the number of strange quarks observed in hadrons (assuming that no new strange quarks are created by resonance decays), and, based on measured resonance rates and known decay multiplicities, estimates analytically the number of primary particles. The strange-hadron count includes charged and neutral kaons, lambdas, and eta's, the latter weighted by 0.5, to account for the $\approx 50\%$ $s\bar{s}$ -component in their wave function. Small

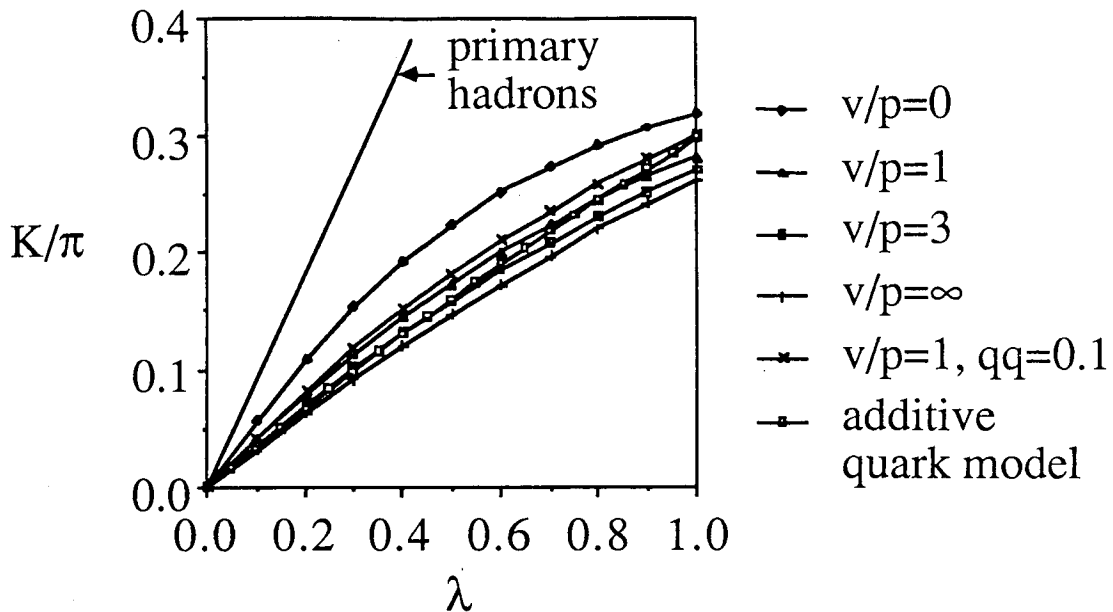


FIGURE 8

Ratio of charged kaons to pions as a function of the strangeness-suppression λ , for different ratios v/p of vector mesons to pseudoscalar mesons among the primary hadrons. The $v/p = 1$ predictions also shown for the assumption of occasional baryon production among primaries, implemented following the Lund diquark scheme⁵ and using $qq/q = 0.1$. The results are derived analytically taking into account the known decay chains. The line indicates the ratio of strange to non-strange primary particles.

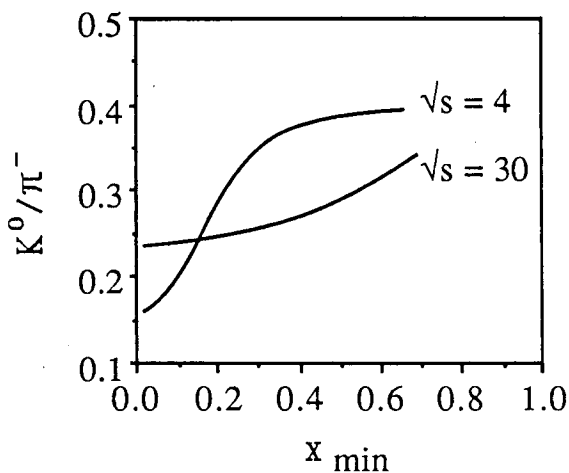


FIGURE 9 (a)

Prediction of the Lund Monte-Carlo generator²² for the ratio of inclusive K^0 and π^- cross sections for $x > x_{\min}$ in the d-quark jets, for energies W of the hadronic system of 4 GeV and 30 GeV. The simulation used $\lambda = 0.30$. In the limit $x_{\min} \rightarrow 1$, the ratio should approach λ .

corrections are applied for the strange baryons which have neither kaon nor lambda in their decay chains. When applied to $u\bar{u}$ events from a Monte-Carlo generator²² (using $\lambda = 0.30$ as input), the technique overestimates λ considerably (Fig. 9 (b)). The reason is simple: even though eta mesons contain strange quarks, they can be generated (via their $u\bar{u}$ and $d\bar{d}$ components) even for $\lambda=0$. An eta meson is thus not necessarily equivalent to 0.5 produced $s\bar{s}$ pairs!

A final problem in the case of e^+e^- annihilation is the large strangeness production in charm and bottom decays, which at present energies account for $\approx 30\%$ of strange-particle yields. Except for the D's, however, decay channels are not well known and the uncertainty on this correction is big. Overestimates in the kaon rate from charm resulted in significant underestimates of λ in some early measurements.

Let us turn to measurements, and first consider strangeness production in e^+e^- annihilation. Fig. 10 shows a compilation²³ of the average number of K^0 's per event as a function of the cms energy \sqrt{s} , compared to predictions of the Lund model⁵ for $\lambda = 0.3$. Also indicated are the contributions from primary strange quarks and from decays of charmed and bottom hadrons, which are of course energy-independent, except for thresholds. We notice that the model represents the energy dependence of the K^0 rate reasonably well using $\lambda = 0.3$. Various e^+e^- experiments^{12,23-26} have measured λ at fixed \sqrt{s} ; their λ values are in most cases obtained from fits of Lund model predictions to K and π inclusive cross sections, and are summarized in Fig. 11(a). Here as well as in the following figures, the error bars are of limited significance, since some experiments give just the statistical errors, whereas others include the effects of uncertainties in (some) other model parameters, which influence the measured λ . Few analyses study the effects of variations of all model parameters within experimental limits, or discuss the dependence of the measured λ on the hadronization model. Realistic systematic errors for most results are in the neighborhood of 20% or more.

Strange-particle production has also been studied extensively in lepton-nucleon scattering²⁷⁻³². There, the identity of the frag-

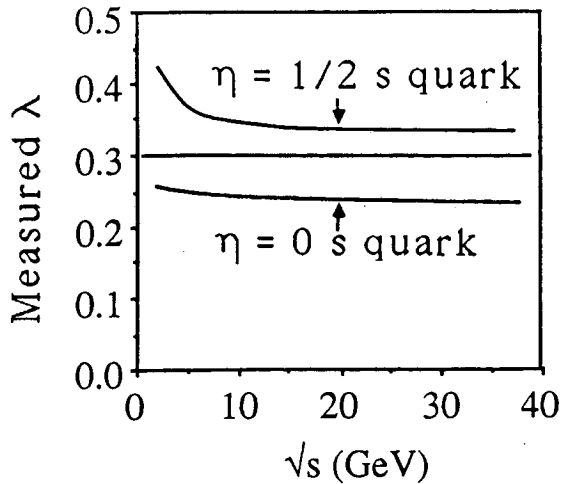


FIGURE 9 (b)

The value of λ reconstructed from Monte-Carlo generated e^+e^- annihilation events using Wroblewski's hadron-counting technique, for different center-of-mass energies. λ was calculated by counting η mesons as containing 0.5 strange quarks. Also shown is the result obtained if η mesons are counted as 0 strange quarks. The generator used a constant value $\lambda = 0.3$.

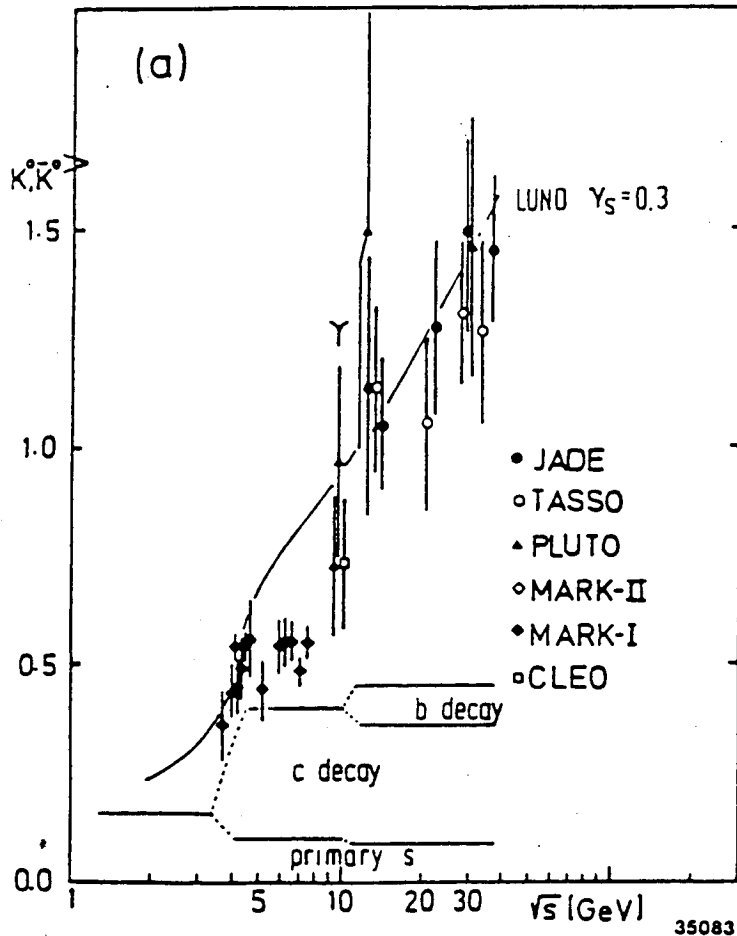


FIGURE 10

Average number of neutral kaons per e^+e^- annihilation event as a function of the center-of-mass energy \sqrt{s} . Also shown is the prediction by the Lund Monte Carlo generator for $\lambda = 0.3$, and the contributions due to primary strange, charm and bottom quark pairs.

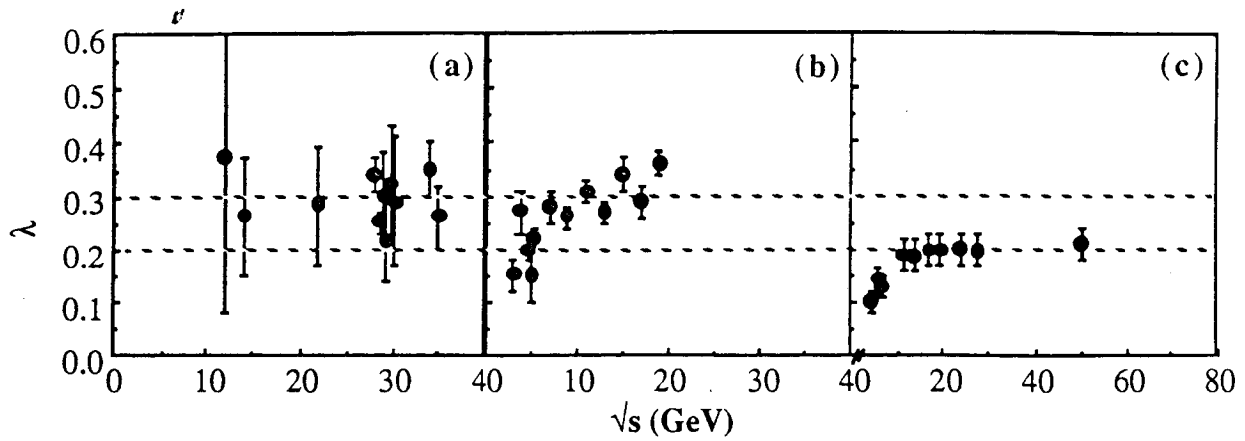


FIGURE 11

(a) Measured values of λ as a function of center-of-mass energy, for e^+e^- annihilation events^{12,23-26}, (b) for deep-inelastic lepton-nucleon scattering²⁷⁻³² and (c) for proton-proton reactions¹⁷. Not all errors include systematics (see text).

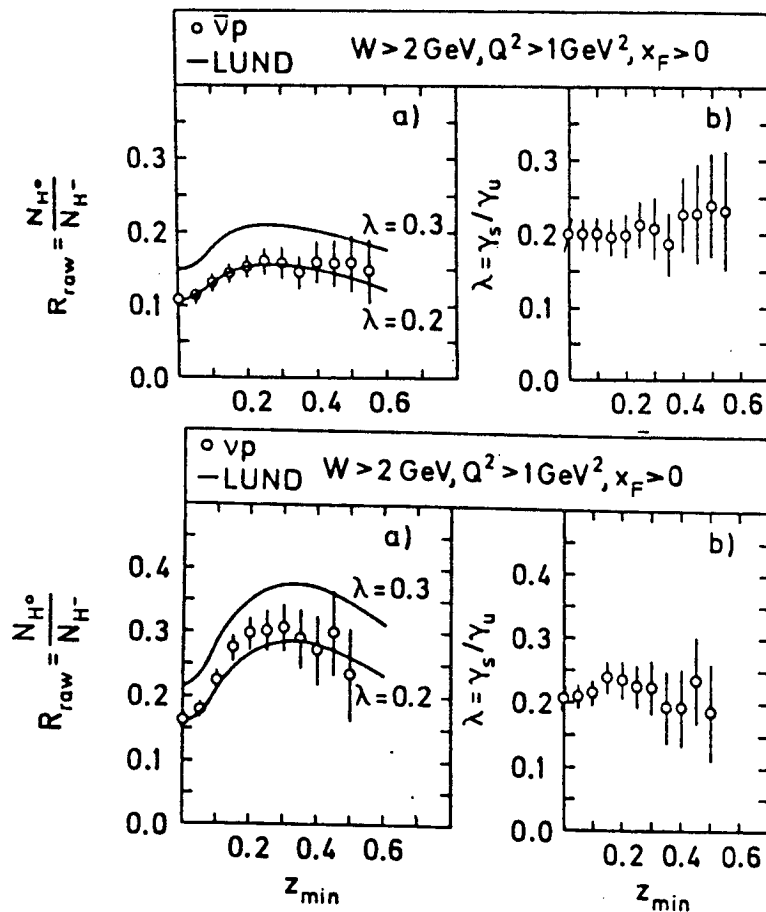


FIGURE 12

(a) The uncorrected ratio of neutral kaon rate and rate of negative hadrons as a function of z_{\min} , for vp (bottom) and $\bar{v}p$ (top) events²⁷. Curves show the predictions of the Lund Monte Carlo for $\lambda = 0.2$ and $\lambda = 0.3$. (b) The values of λ obtained by linear interpolation from the Monte-Carlo curves in (a), vs z_{\min} .

menting quark is (at least approximately) known, and λ is usually determined in the current fragmentation region. For fast hadrons, the ones most likely to contain the scattered quark plus another newly created quark, the strange/non-strange ratio provides a rather direct measurement of λ (see also Fig 9 (a)). Fig. 12 shows data from BEBC²⁷: the ratio R of the K^0 production rate to the rate of negative hadrons as a function of the minimum z above which particles are included in the analysis. z is defined as the ratio of hadron and scattered quark momentum; requiring high z should select leading hadrons. In Fig. 12, R is compared with Lund model predictions for different λ and the optimum value of λ is derived by interpolation. Both the vp and $\bar{v}p$ data point to $\lambda \approx 0.2$; the λ values derived for the two data sets are consistent with each other and largely independent of the cut in z. Fig. 13 demonstrates further that the same λ is obtained for samples with different Bjorken-x, momentum transfer Q^2 , final-state mass W, charged multiplicity, or transverse momentum p_T of a particle. This indicates that the Lund model does provide a consistent description of the data. As a final result, $\lambda = 0.203 \pm 0.014(\text{stat}) \pm 0.010(\text{syst})$ is quoted; the systematic error refers to acceptance uncertainties and variations in some of the model parameters. The authors note that even at high z differences between the full Lund Monte Carlo simulation and simplified analytical models are of the order 30%, a fact neglected e.g. in the analysis of ref. 28, where a higher value $\lambda = 0.27 \pm 0.04$ is obtained, while measured particle ratios are consistent with the BEBC data.

In deep-inelastic muon-proton scattering at somewhat higher average W, the EMC collaboration²⁹ finds $\lambda \approx 0.30 \pm 0.01(\text{stat}) \pm 0.07(\text{syst})$, using basically the same Lund model and similar fitting techniques as for the BEBC data (Fig. 14). The λ -values obtained in lepton-nucleon scattering as a function of the invariant mass W of the hadronic system are summarized in Fig. 11(b).

Finally, consider hadronic reactions. I will first try to demonstrate in a rather model-independent way that there are no drastic differences in the strange-particle production rates between low- p_T

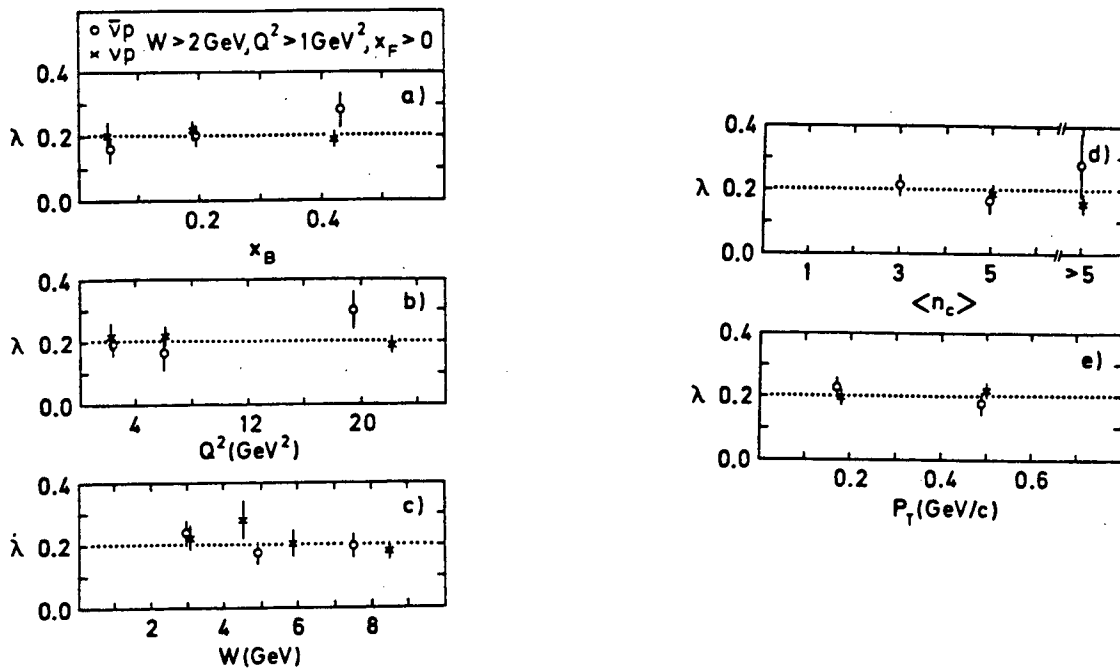


FIGURE 13

The interpolated λ at $z_{\min} = 0$ for νp and $\bar{\nu}p$ scattering as a function of (a) x_B , (b) momentum transfer Q^2 , (c) hadronic mass W , (d) total charged multiplicity $\langle n_c \rangle$ and (e) transverse momentum p_T of the hadrons. The horizontal dotted lines show $\lambda = 0.20$ which is the average value determined from the combined data sample²⁷.

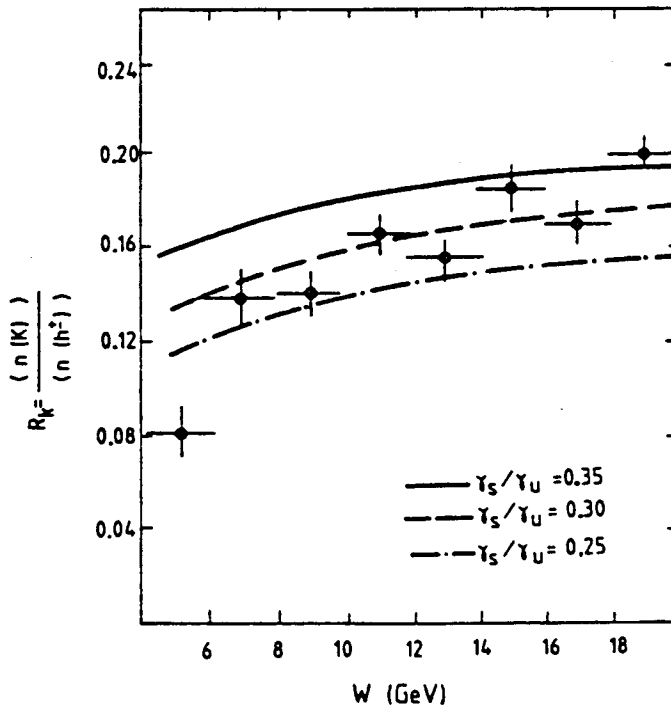


FIGURE 14

Ratio of the average total kaon multiplicity to the total charged particle multiplicity as a function of the mass W of the hadronic system generated in deep-inelastic muon-nucleon scattering reactions²⁹. The curves show Lund model predictions for λ values of 0.25, 0.30 and 0.35.

hadronic reactions and large- q^2 processes such as e^+e^- annihilation. We compare in Fig. 15 the K/π ratio in pp and $p\bar{p}$ interactions³³ and in e^+e^- annihilation at PEP³⁴. In order to stay away from the highly process-specific fragmentation regions, data from the central region $y \approx 0$ is used. While the e^+e^- data point falls slightly above the pp data, it is consistent within errors, in particular given the discrepancies between different pp experiments -- an indication that their systematic errors might be underestimated. One should further note that in hadronic collisions about half of the incident energy is carried away by leading baryons and does not contribute to the production of new particles; particle production in pp collisions at a given $\sqrt{s_{pp}}$ should be compared to e^+e^- annihilation at $\sqrt{s} \approx \sqrt{s_{pp}}/2$. Wroblewski²¹ has compiled data from hadronic reactions (using the hadron-counting technique discussed above) and has derived the λ values shown in Fig. 11(c). His method (where phase-space effects are included in λ) yields $\lambda \approx 0.2$, with little energy dependence once the cms energy exceeds 10 GeV (corresponding to 5 GeV or less actually available for particle production). On the other hand, another compilation³⁸ derives $\lambda = 0.30 \pm 0.02$ from basically the same data, albeit using somewhat oversimplified techniques. The discrepancy between those analyses once more points to the fundamental crux of all λ measurements -- the strong dependence on model assumptions.

The totality of the data presented above points to a value of λ around 0.2-0.3, without unambiguous evidence for a dependence on reaction type or cms energy, given the systematic errors of order 20-30%.

The λ value of about 0.2-0.3 has a quite natural interpretation in the flux-tube model^{2,4-7} discussed above. Its basic assumption - a quasi one-dimensional confinement force field - is consistent with spectroscopic data and supported by the attempts to simulate confinement on a lattice³⁵. If in such a color force field a quark-antiquark pair appears at one point along the string, energy conservation is violated by $2m_q$ and the system is in a short-lived, virtual state. If the quark pair has the right color to screen the initial color field, and if the quarks manage during their lifetime

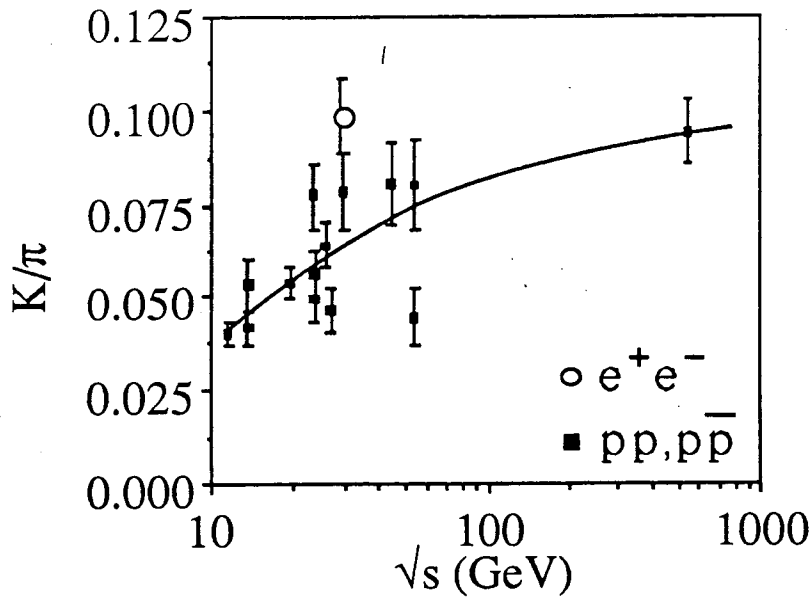


FIGURE 15
Ratio of kaon to pion cross sections in the central rapidity region of pp and $p\bar{p}$ interactions³³, and for e^+e^- annihilation events³⁴, as a function of the center-of-mass energy \sqrt{s} .

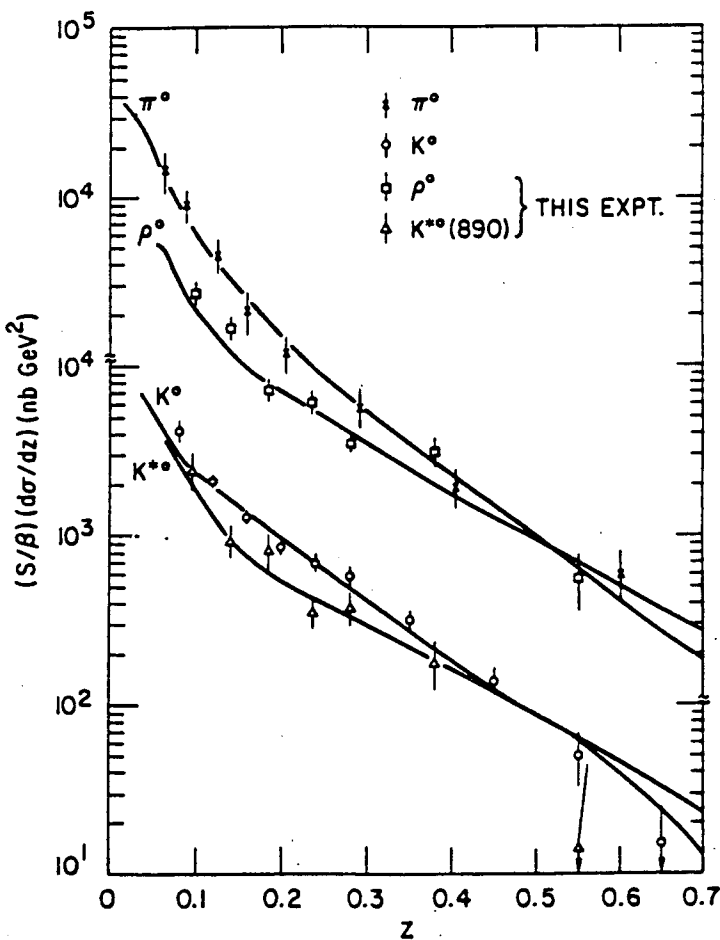


FIGURE 16
Scaled cross section for production of π^0 , K^0 , ρ^0 and $K^{*0}(890)$ in e^+e^- annihilation at $\sqrt{s} = 29$ GeV³⁶. Charge conjugate states are included, where applicable. The curves show Lund model predictions for $\lambda = 0.34$.

$\Delta t \approx 1/2m_q$ to separate far enough to screen an amount of field corresponding to $2m_q$, the quarks may end up on-shell and the string is broken. The process is basically a tunneling phenomenon, and the quark production rate depends strongly on the size of the barrier, i.e. on the mass of the newly formed quarks. One finds:

$$\text{quark production rate} \approx \exp\left(-\frac{\pi m_q^2}{\kappa}\right) \quad (4)$$

Since the quarks are confined within a color flux tube with transverse dimensions similar to typical hadron sizes, the general expectation is that constituent quark masses of about 350 MeV for up and down quarks and of 500 to 550 MeV for strange quarks should be used. With these masses, we can solve Eqn. (4) for the energy per unit length of the string, κ . One finds a values of κ around 1 GeV/fm, well consistent with the nominal value of about 0.9 GeV/fm (corresponding to a confining force between quark and antiquark of about 10 tons) derived from the slope of Regge trajectories and other observations². Given that value of κ , charm and bottom quark rates are suppressed by many orders of magnitude compared to light quarks.

At this point I should come back to an earlier remark, namely the question if the strange particle suppression can really be attributed to a constant strangeness suppression factor at the quark level. In other words, do such models really give a consistent description of the data? We have already seen (Fig. 13) that within one experiment a fixed value of λ describes the data over a wide range of kinematical variables. Further checks include

- The comparison of λ as determined from the K/π ratios, from the ratio of strange to non-strange charmed mesons and from the ratio of strange to non-strange bottom mesons. Such a comparison tests the flavor-independence of the recombination of quarks into mesons. Unfortunately, no experimental data is available so far.
- Consistency between K/π and K^*/ρ . Within the experimental precision of about 15%, data on K, π, K^*, ρ ³⁶ are indeed well described by models with a constant λ (see Fig. 16). (String models suggest⁵ that the ratio v/p of vector meson production to pseu-

doscalar meson production may be different for light and heavy quarks, complicating the interpretation of the data somewhat. However, the variation of v/p between u,d and s quark states should be insignificant compared to present experimental errors).

- Consistency between ϕ/K^* and K^*/ρ . The suppression factor for the second strange quark should be the same as for the first one. Again models are indeed consistent with experiments³⁷ (Fig. 17), however the experimental errors are sizable.
- Consistency between Λ/p and K/π . The same suppression factor should describe both the meson and the baryon sector. However, given our limited knowledge of mechanisms of baryon production, this test relies strongly on phenomenological models; we will return later to this subject.

Let me try to summarize the results mentioned so far:

- At the level of pseudoscalar mesons and vector mesons as primary particles, production of strange quarks in hadronization processes is suppressed compared to u quarks by a factor 0.2-0.3.
- The precise value of λ is quite model dependent; a perfect determination of λ requires knowledge of the cross sections and decay modes of all resonances feeding into stable hadrons.
- Given all these problems, there is no evidence for a reaction dependence or an energy dependence of λ (once one is well above threshold).
- The numerical value of λ finds a "natural" explanation in the framework of color string models. It should be obvious, however, that due to the somewhat arbitrary choice of the effective quark masses the significance of this observation is limited.

Finally, I want to mention some alternative approaches and one outstanding problem. As indicated before, it is not obvious that the primary objects produced in fragmentation processes are the familiar ground state mesons and baryons. Models¹⁶⁻¹⁹ with primary hadronic clusters of average mass around 2-3 GeV, decaying into two mesons, another cluster and a meson or two light clusters are capable of describing the experimental data quite well. Since a typical cluster will give rise to several mesons, the number of primary clusters in an event is significantly smaller than the equivalent

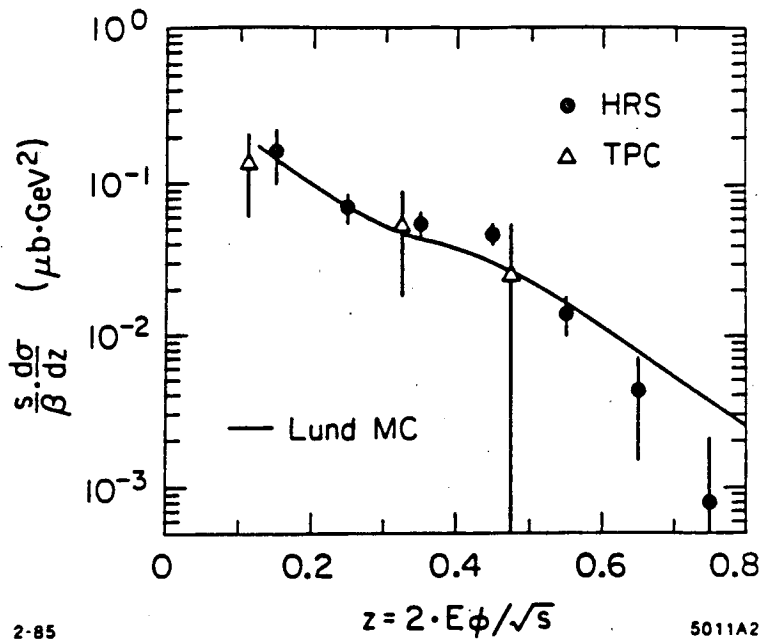


FIGURE 17

Scaled cross section for ϕ production e^+e^- annihilation at $\sqrt{s} = 29$ GeV³⁷, again compared to Lund model predictions (the model calculation uses approximately the same value of λ as the one shown in Fig. 16).

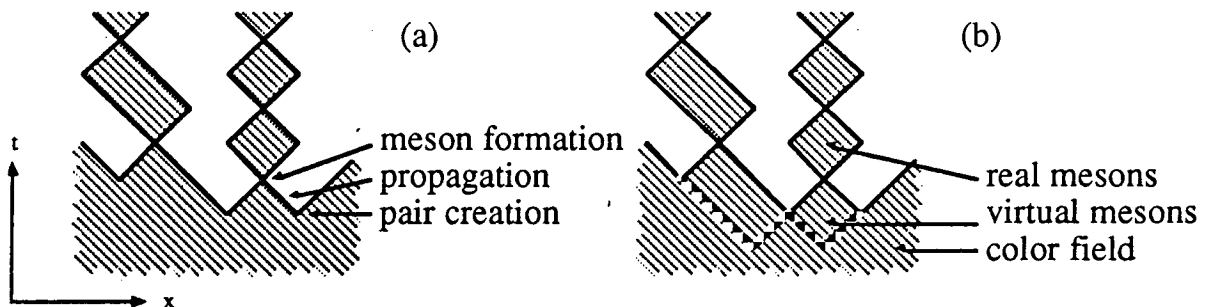


FIGURE 18

Space-time diagrams describing hadron production in string models: conventional formulation based on the string \rightarrow quarks, quarks \rightarrow mesons transition in a one-dimensional system of massless quarks (a) and alternative description as a direct transition strings \rightarrow mesons (b).

number of primary mesons e.g. in the Lund model. On the other hand, for cluster masses in the few-GeV range, strange-particle production is still significantly suppressed by phase space, and the number of final strange hadrons is still close to the number of strange clusters. As a consequence, less strangeness suppression is needed at the cluster level; models typically use $\lambda \approx 0.6-0.8$ in order to describe the data.

One may also question another assumption built into the models with a fixed strangeness suppression parameter λ : in a quantum mechanical system such as a color string, it is hard to see why the particle production process can be factored into two stages, namely quark pair production in the color field and successive recombination. Both processes occur on similar time scales and interference effects should be significant. After all, the newly produced quarks "fall" immediately into a bound meson state. These arguments, which are used to justify e.g. the suppression of spin-1 mesons⁵, are represented in Fig. 18. The figure shows the usual space-time diagram describing quark pair production in the string, propagation of quarks until they meet a partner, and then propagation in a "yoyo" mode as a bound meson (Fig. 18(a)). Equally well, one can however view the stage of propagation of the quark as part of the first oscillation of the meson "yoyo" (Fig. 18(b)); from this point of view it appears that the color flux tube as a whole undergoes a transition into meson states, without an intermediate quark stage. Of course, due to the uncertainty relation the two views cannot really be distinguished, but the question remains as to which (if any) is the more appropriate classical description. In the normal string models, the inclusive cross section for a hadron H_i is:

$$\left(\frac{d\sigma}{dy dp_T^2} \right)_{\text{central region}} \sim g(p_T^2) P(q_i) P(\bar{q}_j) |\langle H_i | q_i \bar{q}_j \rangle|^2 \quad (5).$$

The p_T distribution g , the quark production probabilities P and the overlap integral between $q\bar{q}$ and hadron wavefunction contain ad-hoc parameters such as λ . In the spirit of Fig. 18(b), one might

speculate that hadron production rates might depend only on the energy (to be precise, on the transverse energy $E_T = \sqrt{m^2 + p_T^2}$) required to create the hadron (i.e., the length of string used up in the process), and on SU(3) Clebsch-Gordan coefficients. String-model arguments suggest an $\exp(-bE_T^2)$ dependence (the actual expression is slightly more complicated). One and the same constant accounts for the suppression of large transverse momenta, of vector mesons, of strange mesons and of baryons. Such a modification of the Lund string model has been studied in Ref. 40. More or less by construction, the model retains inclusive distributions predicted by the Lund model. Amazingly enough, it predicts hadron rates for non-strange and strange mesons and baryons correctly within about 30-40%, over a range of more than 3 orders in magnitude between frequent (π) and very rare (Ω) particles (Fig. 19). Transverse-momentum spectra are also reproduced well. While there are certainly open questions as to the details of the implementation of this model, it demonstrates that present data cannot be used to prove conclusively that the suppression of strange hadrons actually occurs at the quark level. Much more precise measurements of production rates are needed for a better distinction!

The open problem concerns the production rate of strange mesons from scattered valence quarks in proton-proton interactions. A SFM experiment⁴¹ measured the K/π ratio at large- p_T in a kinematic regime where the source of hadrons is almost certainly the large-angle scattering of a valence quark. In this case, the K/π ratio is again directly related to λ . However, the experiment finds a K/π value of 0.50 (Fig. 20), in agreement with earlier experiments at lower energies. The large K/π ratio can require a λ of 0.55 ± 0.05 , in disagreement with the results discussed above. We can only speculate about a source of this disagreement. Since in the ISR data ISR pions and kaons carry a large fraction (about 80%) of the quarks momentum (due to the "trigger bias"), one could assume a z -dependence of λ ⁴². Since the production of large- z particles involves sizable momentum transfers, it is not unnatural to assume that the importance of mass effects is diminished. However, the neutrino experiment²⁷ discussed above finds no such dependence, and

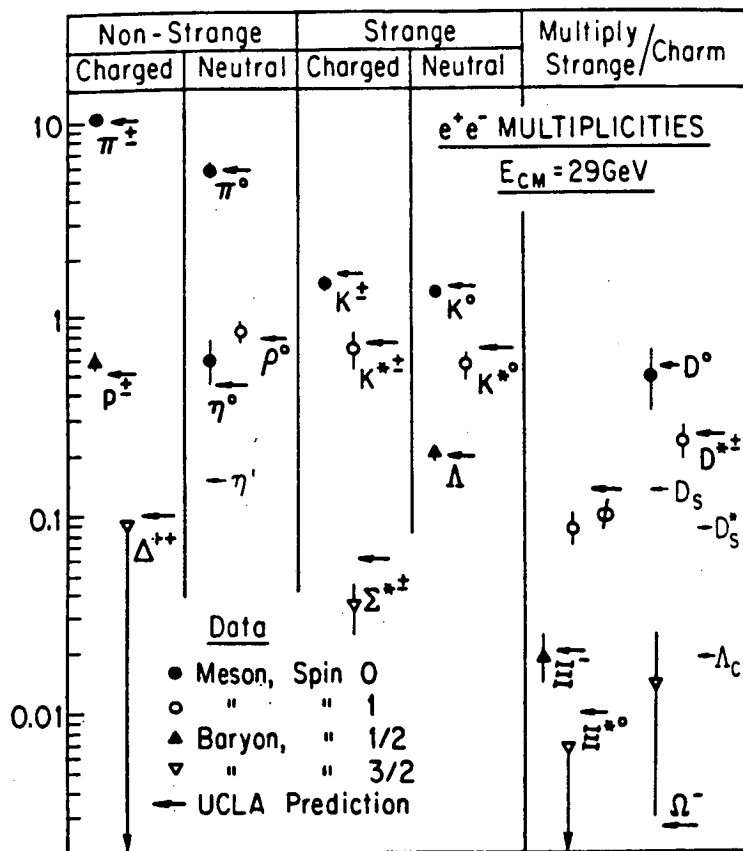


FIGURE 19
Comparison of experimental multiplicities with the predictions of the model of ref. 40 for various hadron flavors created in e⁺e⁻ annihilation at $\sqrt{s} = 29$ GeV. Anti-particles are included in all cases.

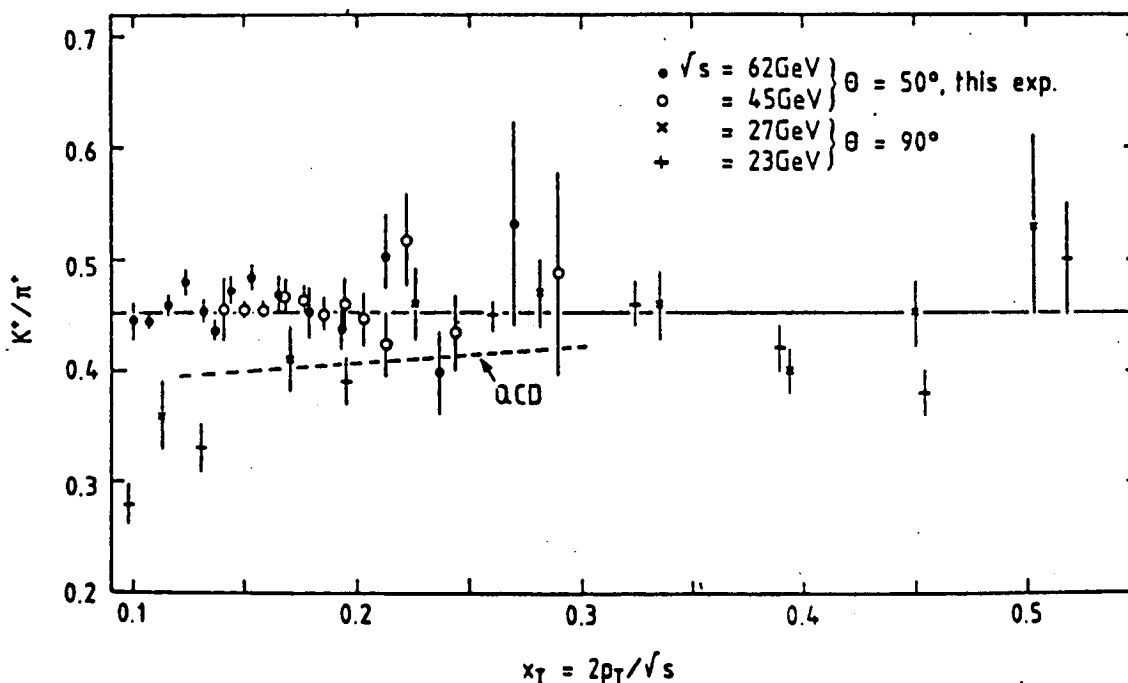


FIGURE 20
Experimental ratio of K⁺ to π⁺ production in proton-proton interactions at large $x_T = 2p_T/\sqrt{s}$ ⁴¹. The dashed line shows a model prediction using $\lambda = 0.5$

the neutrino data and the ISR experiment appear to be inconsistent (Fig. 21). One remote possibility is that λ does indeed increase with z , but that at the relatively low W of the νp data this rise is offset by phase space effects. Another explanation is that there is another source of kaons in the ISR high p_T data besides quark fragmentation. For example, it was recently pointed out⁴³ that higher twist contributions (i.e. direct meson production) play a significant role for some particle species (although at least for the calculation of ref. 43 and the kinematic region considered there, the increase in the kaon yield due to higher twists is relatively small). Precise measurements of particle fractions in e^+e^- annihilation events at 29 GeV cms energy will soon be available⁴⁴ and may help to solve this puzzle.

3. STRANGENESS PRODUCTION MECHANISMS AND CORRELATIONS BETWEEN STRANGE PARTICLES.

In the investigation of parton fragmentation, the study of particle correlations can give information beyond that obtainable from inclusive spectra. As discussed in the introduction, the strangeness quantum number can be used to label a specific quark pair and to study the effect of confinement forces on those quarks. Typically, correlations are studied in the following way: one selects events with a "test particle", say a K^- , in a small, fixed rapidity interval, and then in those events considers the number of additional kaons produced as a function of their rapidity, or as a function of the rapidity difference to the "test" kaon. Fig. 22 shows KK correlation functions in e^+e^- annihilation events⁴⁵ and in hadronic interactions⁴⁶. In each case, the correlation function is defined as the measured number of additional kaons per event divided by the number of kaons found in the same kinematic interval in average events without the "test kaon" requirement:

$$C = \left(\frac{1}{\sigma} \frac{d^2\sigma}{dy_K dy_{\text{test}}} \right) / \left(\frac{1}{\sigma^2} \frac{d\sigma}{dy_K} \frac{d\sigma}{dy_{\text{test}}} \right) - 1 \quad (6).$$

This definition yields $C=0$ for uncorrelated production. We observe a strong positive correlation of opposite-sign kaons at small rapidity differences. The positive correlation is simply a reflection

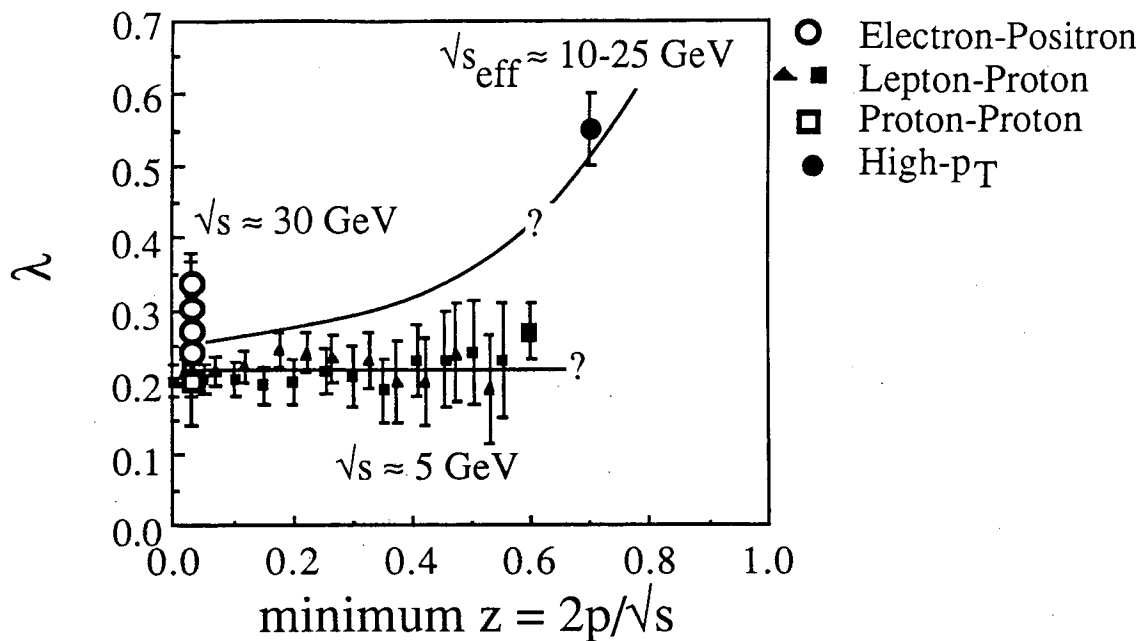


FIGURE 21

Values of λ as derived from K/π ratios, as a function of the minimum $z = p_{\text{hadron}}/p_{\text{quark}}$ above which hadrons are used in the analysis. Data are shown for e^+e^- annihilation (from several experiments), for neutrino-nucleon scattering, for low- p_T pp reactions and for high- p_T meson production in pp interactions.

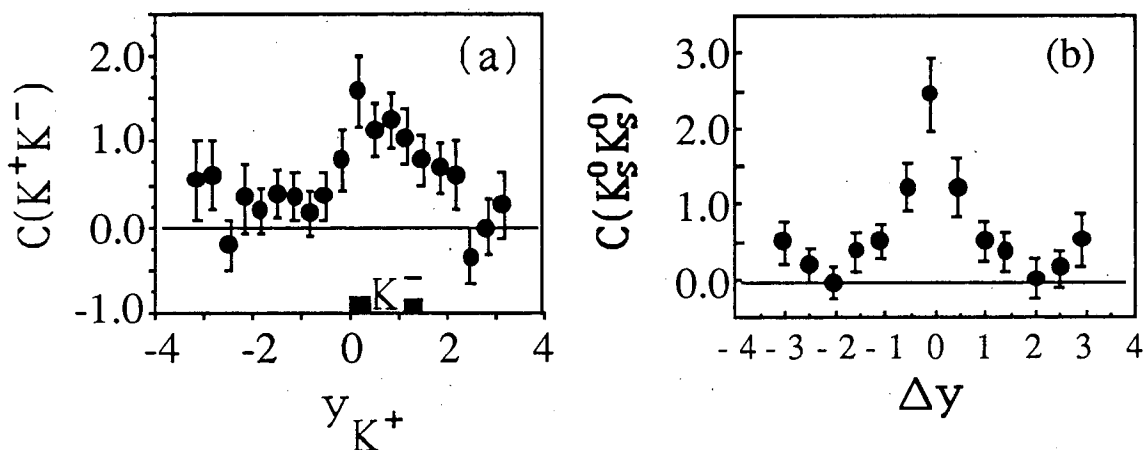


FIGURE 22

(a) Correlation function C for unlike-sign kaon production in e^+e^- annihilation events at $\sqrt{s} = 29$ GeV⁴⁵, as a function of the rapidity of one kaon, while the other one is fixed in the interval $0 < y < 1.5$. (b) Correlation between neutral kaons produced in hadronic interactions, as a function of the rapidity difference⁴⁶.

of strangeness conservation; however the fact that the excess of opposite-sign kaons is localized at the same rapidity as the test particle indicates that confinement does indeed involve only small momentum transfers and does not separate quark pairs over large distances in phase space (i.e. rapidity).

An interesting result is obtained if the test particle is moved towards high rapidity into the fragmentation region of e^+e^- events (Fig. 23). Now there are indications of two peaks in the correlation function, one local peak and one peak at large and opposite rapidity, indicating that two different mechanisms contribute to the production of strange-quark pairs: one low- q^2 mechanism and one mechanism creating large rapidity separations, i.e. large momentum transfers. Of course, the latter mechanism is the initial hard process creating the primary quark-antiquark pair from the virtual photon: $s\bar{s}$ or $c\bar{c}$ pair production result in events with particles of opposite strangeness in the two fragmentation regions. The low- q^2 process is then the color confinement; in this case the strange quarks are produced from the breakup of the color field.

These kaon correlations are consistent with expectations based on the string model; however they do not prove conclusively that hadronization does indeed proceed along a quasi-onedimensional string. A correlation effect more characteristic for string models was observed recently⁴⁷ in a study on baryon correlations: in string models, the rapidity y of a particle is closely related to the position of the production points of its partons along the string. It is hence difficult to create particles with identical quantum numbers (such as charge, strangeness, or baryon number) at the same rapidity. Both along the string and in y the signs of quantum numbers tend to alternate; a strange particle is followed by an anti-strange particle, a baryon by an antibaryon etc. String models therefore predict an anticorrelation between two like-sign pions, kaons, or protons. Unfortunately, this anticorrelation is virtually unobservable for pions, since most π 's result from resonance decays, and (anti-)correlations are washed out, and since Bose-Einstein correlations further enhance production of pion pairs with small momentum differences. The anticorrelation is observed

for baryons⁴⁷, where resonance smearing plays a negligible role (Fig. 24(a)). A similar (however somewhat weaker) anticorrelation shows up for like-sign kaons produced in 2-jet events (Fig. 24(b)). For this analysis, 3-jet events with radiative gluons have been explicitly excluded, since an additional large-angle jet gives rise to very strong correlations, completely wiping out the weak anticorrelation. The like-sign "repulsion" is not as pronounced for kaons as it is for protons (where it is visible without additional cuts); indeed string models predict the effect to increase with rising hadron mass⁴⁷.

In summary, string models provide a surprisingly good phenomenology of not only of inclusive strange-particle production, but also of correlations between strange particles.

4. BARYON PRODUCTION

As outlined earlier, baryons offer additional degrees of freedom, which are valuable in a systematic study of confinement processes. At this point, the only models of baryon production which have survived the experimental tests are the diquark model and its variants⁴⁸⁻⁵². These models assume that occasionally a diquark-antidiquark pair is produced in the confinement process. Since a diquark can act as an effective color antitriplet, it may combine with a quark to form a baryon. So far, it is not completely clear if such diquarks represent tightly-bound objects or if two loosely-interacting quarks merely act as some kind of "effective diquark". Diquark models predict^{48,49} a strong suppression of baryons with spin-1 diquarks, or with strange diquarks, since diquark creation rates in a color field depend exponentially on the square of the diquark mass - see Eqn. 4. A strange diquark is hence more strongly suppressed (compared to a non-strange diquark) than a strange quark (compared to a non-strange quark). While the notion of pointlike diquarks may seem far fetched, detailed mechanisms have been described³ of how effective diquarks can form. Baryon production is best studied in processes without incident baryons, such as e^+e^- annihilation. While many papers on proton and Λ production in high-energy e^+e^- interactions at PEP and PETRA energies have been pub-

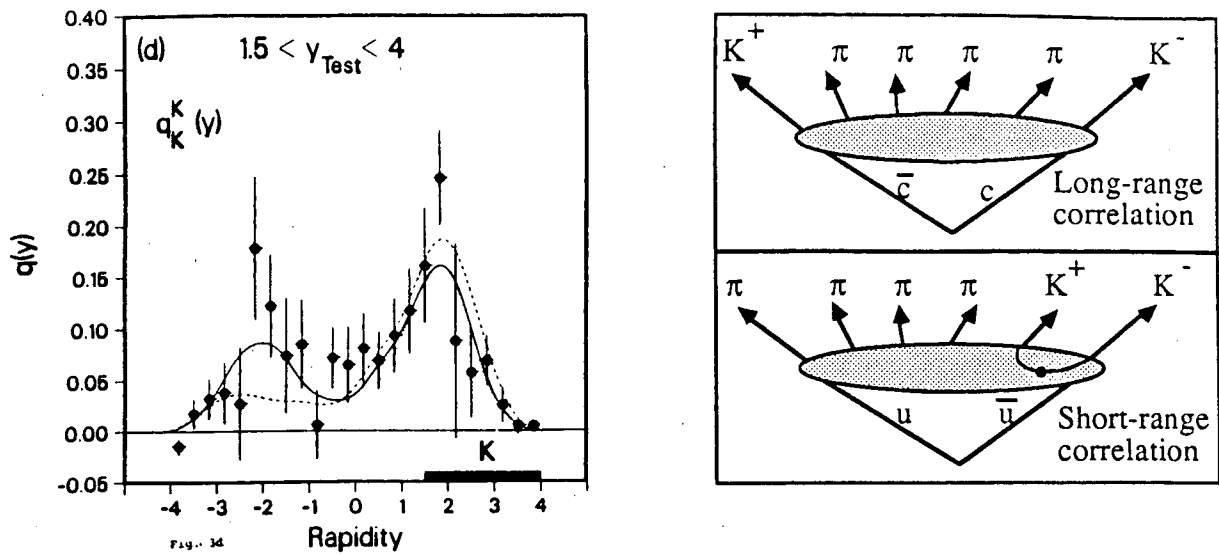


FIGURE 23

Net strangeness per unit rapidity seen in charged kaons, for e^+e^- annihilation events with a selected K^- at large rapidity $y > 1.5$ 45. The quantity shown measures where in rapidity the strangeness of the K^- is compensated and is roughly equivalent to the difference between the correlation functions for opposite-sign and like-sign kaon pairs. The curves show predictions of different fragmentation models. The diagram to the right indicates the sources of long-range and short-range kaon correlations.

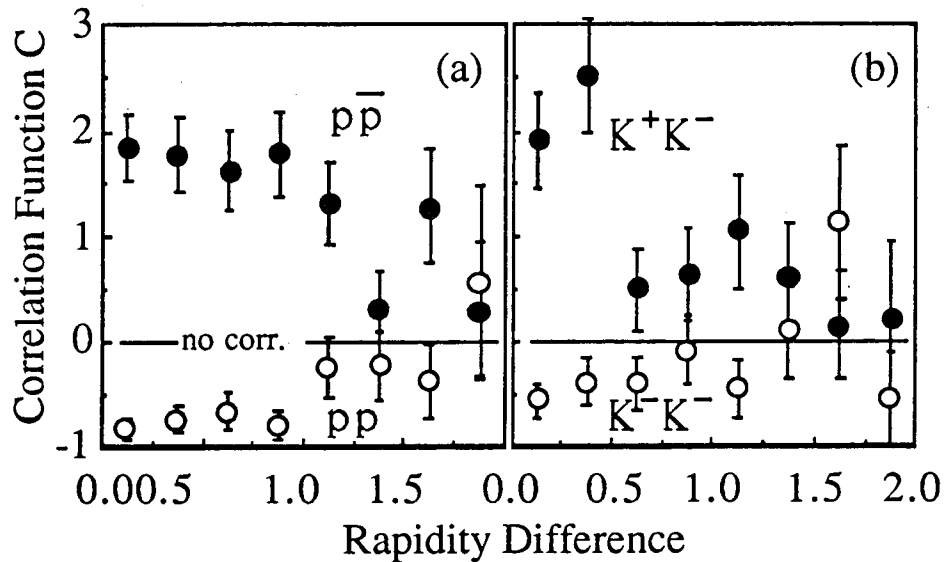


FIGURE 24

(a) Correlation function C for proton-antiproton pairs and for proton-proton pairs in e^+e^- annihilation events at $\sqrt{s} = 29$ GeV 47, as a function of the rapidity difference between the two baryons. (b) same for unlike-sign and like-sign kaon pairs in 2-jet events.

lished^{14,53-55}, the most concise data set on strange baryon production comes from the ARGUS experiment⁵⁶ at the DORIS storage ring. In order to extract strangeness suppression etc., I fitted the ARGUS data using a diquark model with SU(6) symmetry broken by suppression factors for spin-1 diquarks and for strange diquarks⁵⁸. For λ -values in the range discussed before, $\lambda=0.2-0.3$, this model works quite well and yields a strange-diquark suppression considerably bigger than λ : $P(us_0)/P(ud_0)=0.10\pm 0.04$ (the index 0 indicates the diquark spin). As expected, all spin-1 diquarks are found to be suppressed by at least a factor 50 compared to the lightest diquark, a spin-0 ud system.

5. POLARIZATION

Both string models and QCD calculations predict significant polarization effects in the hadronization process; basically, baryons should be polarized perpendicular to the transverse momentum of the hadron and to the direction of the color field⁴⁹. Such polarization is indeed observed for leading baryons in hadronic collisions, and is consistent with the predictions³⁹. A quite complete discussion of polarization effects in hadronic reactions can be found elsewhere in these proceedings; I will not repeat the discussion here. Detection of baryon polarization in e^+e^- annihilation, where the configuration of the color field is (theoretically) much better known would provide a further excellent test of string models. Unfortunately, measurement of the polarization requires knowledge of the color field direction, i.e. knowledge as to which jet is the quark jet and which the antiquark jet. Algorithms to identify these jets have been developed, but so far only upper limits on Λ polarization have been given⁵². It is at this point not clear whether these limits are in contradiction with model predictions or not.

6. SUMMARY

In summary, one can state that the production of strange hadrons in high-energy reactions provides an extremely valuable and not yet fully exploited tool to study the dynamics of flavor production in confinement processes. So far, the one-dimensional color string

provides a rather convincing phenomenology of hadron production in general, and of strange particle production in particular. Although in typical implementations of the string model strangeness suppression factors are treated as free parameters, the resulting values of the parameters can be explained in terms of quark mass effects. However, more and better measurements are needed to rigorously test model predictions beyond the present 10-20% level of accuracy.

DISCLAIMER

This paper is supposed to serve as an introduction to the topic, it is not exhaustive as far as the discussion of data and models or the list of references is concerned. Emphasis is placed on strangeness production in quark fragmentation and its description in the very popular framework of string models; because of length limitations, many interesting related topics, such as the discussion of beam and target fragmentation in hadronic reactions, or of alternative models for hadron production are omitted or abbreviated.

ACKNOWLEDGEMENTS

This work was supported by the U.S. Department of Energy under Contract No. DE-AC03-76SF00098 and by the National Science Foundation. The author acknowledges receipt of an A.P. Sloan Fellowship.

REFERENCES

- 1) J. Schwinger: Phys. Rev. 82, 664
- 2) A. Casher, H. Neuberger, S. Nussinov: Phys. Rev. D20 (1979) 179
- 3) A. Casher, H. Neuberger, S. Nussinov: Phys. Rev. D21 (1980) 1966
- 4) H. Neuberger: Phys. Rev. D20 (1979) 2936
- 5) B. Andersson et al.: Phys. Rep. 97 (1983) 31
- 6) E. Brezin, C. Itzykson: Phys. Rev. D2, 191 (1970)
- 7) E.G. Gurvich: Phys. Lett. 87B (1979) 386
- 8) G. Schierholz, M. Teper: Z. Phys. C13 (1982) 53
- 9) K.W. Bell et al.: RL-820-011 (unpublished)

- 10) B. Andersson, G. Gustafson, G. Ingelman: Phys. Lett. 85B (1979) 417
- 11) J.D. Bjorken: Int. Conf. on Physics in Collision, Stockholm, Sweden, 1982; and FERMILAB-Conf-82/42-THY
- 12) TASSO Collab., M. Althoff et al.: Z. Phys. C22 (1984) 307
- 13) D. Drijard et al., Nucl. Phys. B155 (1979) 269
- 14) TASSO Collab., M. Althoff et al.: Z. Phys. C27 (1985) 27
- 15) V.V. Anisovich, M.P. Kobrinsky: Phys. Lett. 52B (1974) 217
- 16) B.R. Webber: Nucl. Phys. B238 (1984) 492
- 17) T.D. Gottschalk, Nucl. Phys. B214 (1983) 201; B239 (1984) 325; B239 (1984) 349
- 18) G.C. Fox, S. Wolfram: Nucl. Phys. B168 (1980) 285
- 19) R.D. Field, S. Wolfram: Nucl. Phys. B213 (1983) 65
- 20) R. Hagedorn, Proc. Erice 1972, p. 255
- 21) A. Wroblewski, Acta Phys. Pol. B16 (1985) 379
- 22) We used JETSET Vs. 6.3, see T. Sjöstrand, M. Bengtsson: LU-TP 86-22 (1986)
- 23) JADE Collab., W. Bartel et al.: Z. Phys. C20 (1983) 187
- 24) Mark II Collab. H. Schellman et al: SLAC-PUB 3448 (1984)
- 25) HRS Collab.: Phys. Lett. 158B (1985) 519
- 26) TPC Collab.: H. Aihara et al., to be published
- 27) G.T. Jones et al.: Z. Phys. C27, 43 (1985)
- 28) V. Ammosov et al.: Phys. Lett. 93B (1980) 210
- 29) EMC Collaboration, M. Arneodo et al., Z. Phys. C34 (1987) 283
- 30) N.J. Baker et al.: Phys. Rev. D34, 1251 (1986)
- 31) EMC Collaboration, M. Arneodo et al., Phys. Lett. 145B (1984) 156
- 32) I. Cohen et al.: Phys. Rev. Lett. 40 (1978) 1614
- 33) G.J. Alner et al.: Nucl. Phys. B258 (1985) 505
- 34) TPC Collab., H. Aihara et al.: Phys. Lett. B 184 (1987) 114
- 35) C. Petersen, LU-TP 85-15 (1985)
- 36) HRS Collab., M. Derrick et al.: Phys. Lett. 158B (1985) 519
- 37) HRS Collab., M. Derrick et al.: Phys. Rev. Lett. 54 (1985) 2568
- 38) P.K. Malhotra, R. Orava: Z. Phys. C17 (1983) 85.
- 39) K.J. Heller, Proc. High Energy Spin Physics, Marseille (1984)

- 40) C.D. Buchanan, S.B. Chun: UCLA 87-005, subm. to Phys. Rev. Lett.
- 41) A. Breakstone et al.: Z. Phys. C23 (1984) 9
- 42) W. Geist, CERN-EP/87-127, subm. to Phys. Lett. B
- 43) G. Ingelman: DESY 86-131 (1986)
- 44) TPC Collab., H. Aihara et al.: in preparation
- 45) TPC Collab., H. Aihara et al.: Phys. Rev. Lett. 53 (1984) 2199
- 46) R. Harris et al.: Phys. Rev. D18 (1978) 92
- 47) TPC Collab., H. Aihara et al.: Phys. Rev. Lett. 57 (1986) 3140
- 48) B. Andersson, G. Gustafson, T. Sjöstrand: Nucl. Phys. B197 (1982) 45
- 49) B. Andersson, G. Gustafson, T. Sjöstrand: Physica Scripta 32 (1985) 574
- 50) T. Meyer, Z. Phys. C12 (1982) 77
- 51) E.M. Ilgenfritz, J. Kripfganz, A. Schiller: Acta Phys. Pol. B9 (1978) 881
- 52) A. Bartl, H. Fraas, W. Majoretto: Phys. Rev. D26 (1982) 1061
- 53) TPC Collab., H. Aihara et al.: Phys. Rev. Lett. 54 (1985) 274
- 54) P. Baringer et al.: Phys. Rev. Lett. 56 (1986) 1346
- 55) D.H. Saxon, Proc. Int. Conf. on High Energy Physics, Bari (1985)
- 56) ARGUS Collab., H. Albrecht et al.: Phys. Lett. 183B (1987) 419
- 57) CLEO Collab., S. Behrends et al.: Phys. Rev. D31 (1985) 2161
- 58) TASSO Collab., M. Althoff et al.: Z. Phys. C26 (1984) 181

LAWRENCE BERKELEY LABORATORY
TECHNICAL INFORMATION DEPARTMENT
UNIVERSITY OF CALIFORNIA
BERKELEY, CALIFORNIA 94720